

Constraints on Higgs Properties and SUSY Partners in the pMSSM*

M. Cahill-Rowley, J. Hewett, A. Ismail, and T. Rizzo

SLAC National Accelerator Laboratory, Menlo Park, CA, USA[†]

September 26, 2013

Abstract

Direct searches for superpartners and precision measurements of the properties of the ~ 126 GeV Higgs boson lead to important inter-dependent constraints on the underlying parameter space of the MSSM. The 19/20-parameter p(henomenological)MSSM offers a flexible framework for the study of a wide variety of both Higgs and SUSY phenomena at the LHC and elsewhere. Within this scenario we address the following questions: ‘What will potentially null searches for SUSY at the LHC tell us about the possible properties of the Higgs boson?’ and, conversely, ‘What do precision measurements of the properties of the Higgs tell us about the possible properties of the various superpartners?’ Clearly the answers to such questions will be functions of both the collision energy of the LHC as well as the accumulated integrated luminosity. We address these questions employing several sets of pMSSM models having either neutralino or gravitino LSPs, making use of the ATLAS SUSY analyses at the 7/8 TeV LHC as well as planned SUSY and Higgs analyses at the 14 TeV LHC and the ILC. Except for theoretical uncertainties that remain to be accounted for in the ratios of SUSY and SM couplings, we demonstrate that Higgs coupling measurements at the 14 TeV LHC, and particularly at the 500 GeV ILC, will be sensitive to regions of the pMSSM model space that are not accessible to direct SUSY searches.

1 Introduction and Overview of the pMSSM Models

With the discovery of the Higgs boson, the last component of the Standard Model is now in place and searches for new physics continue in earnest. A most important issue with

*White Paper contributed to the Snowmass Community Summer Study 2013, Minneapolis, MN July 29 - August 6, 2013

[†]mrowley, hewett, aismail, rizzo@slac.stanford.edu

respect to the production of new physics at an accelerator is whether or not it can be discovered or excluded given backgrounds arising from the Standard Model (SM), provided it is kinematically accessible. In particular, within a specific model, we would like to know how well a given set of experimental analyses can probe the full parameter space of interest. With the lack of any experimental evidence for new physics so far, this is certainly true in the case of Supersymmetry (SUSY). However, even in the simplest SUSY scenario, the MSSM, the number of free parameters (~ 100) is too large to study in complete generality. The traditional approach is to assume the existence of some high-scale theory with only a few parameters (such as mSUGRA [1]) from which all the properties of the sparticles at the TeV scale can be determined and studied in detail. While such an approach is often quite valuable [2], these scenarios are phenomenologically limiting and are under increasing tension with a wide range of experimental data including the ~ 126 GeV mass of the recently discovered Higgs boson [3, 4]. Of course the discovery of the Higgs boson itself might also provide a new and important window into whatever physics lies beyond the SM. This is certainly true in the case of the MSSM where all of the properties of the Higgs can in principle be calculated perturbatively from the assumed values of the soft breaking parameters in the underlying Lagrangian.

One way to circumvent such limitations is to examine the more general 19/20-parameter pMSSM [5]. The increased dimensionality of the parameter space not only allows for a more unprejudiced study of SUSY, but can also yield valuable information on ‘unusual’ scenarios, identify weaknesses in the current LHC analyses, and can be used to combine results from many independent SUSY related searches. To these ends, we have recently embarked on a detailed study of the signatures for the pMSSM at the 7 and 8 TeV LHC, supplemented by input from Dark Matter (DM) experiments as well as from precision electroweak and flavor measurements [6, 7]. The pMSSM is the most general version of the R-parity conserving MSSM when it is subjected to a minimal set of experimentally-motivated guiding principles: *(i)* CP conservation, *(ii)* Minimal Flavor Violation at the electroweak scale so that flavor physics is controlled by the CKM mixing matrix, *(iii)* degenerate 1st and 2nd generation sfermion masses, and *(iv)* negligible Yukawa couplings and A-terms for the first two generations. In particular, no assumptions are made about physics at high scales, e.g., the nature of SUSY breaking, in order to capture electroweak scale phenomenology for which a UV-complete theory may not yet exist. Imposing these principles decreases the number of free parameters in the MSSM at the TeV-scale from 105 to 19 for the case of a neutralino LSP, or to 20 when the gravitino mass is included as an additional parameter when it plays the role of the LSP. We have not assumed that the LSP relic density necessarily saturates the WMAP/Planck value [8] in order to allow for the possibility of multi-component DM. For example, the axions introduced to solve the strong CP problem may contribute to the DM relic density. The 19/20 pMSSM parameters and the ranges of values employed in our scans are listed in Table 1. Like throwing darts, to study the pMSSM we generate $\sim 3.7 \times 10^6$ model points in this space (using SOFTSUSY [9] and checking for consistency with SuSpect [10]), with each point then corresponding to a specific set of values for these parameters. These individual models are then subjected to a large set of collider, flavor,

precision measurement, dark matter and theoretical constraints [6]. Roughly $\sim 225\text{k}$ models for each type of LSP survive this initial selection and can then be used for further physics studies. Decay patterns of the SUSY partners and the extended Higgs sector are calculated using a privately modified version of SUSY-HIT [11] as well as the most recent version of HDECAY [12]. Since our scan ranges include sparticle masses up to 4 TeV, an upper limit chosen to enable phenomenological studies at the 14 TeV LHC, the neutralinos and charginos in either of the model sets are typically very close to being a pure electroweak eigenstate as the off-diagonal elements of the corresponding mass matrices are at most M_W . This has important implications for the resulting collider and DM phenomenology [13]. Finally, for the neutralino (gravitino) model set we find that roughly $\simeq 20(10)\%$ of the models are found to satisfy $m_h = 126 \pm 3$ GeV; we will focus on these subsets in the analysis that follows¹.

In addition to these two large pMSSM model sets, we have also generated a smaller, specialized neutralino LSP set of $\sim 10.2\text{k}$ ‘natural’ models, all of which predict $m_h = 126 \pm 3$ GeV, have an LSP that *does* saturate the WMAP relic density and produce values of fine-tuning (FT) better than 1% using the Ellis-Barbieri-Giudice measure [14, 15]. This low-FT model set will also be used as part of the present study. In order to obtain this model set we modified the parameter scan ranges listed in the Table to greatly increase the likelihood of both low FT and having a thermal relic density in the desired range. Amongst other things, this requires a bino as the LSP, as well as light Higgsinos and highly mixed stops. We generated $\sim 3.3 \times 10^8$ low-FT points in this 19-parameter space and subjected them to updated precision, flavor, DM and collider constraints as before. Since these requirements were much stricter than for our two larger model sets, only $\sim 10.2\text{k}$ low-FT models were found to be viable for further study.

Within each pMSSM model, the properties of the lightest CP-even Higgs, h , are completely determined as are the corresponding properties of all the superpartners since these follow directly from the chosen values of the soft parameters. This allows us to address the two questions: What will potentially null searches for SUSY at the LHC tell us about the possible properties of the Higgs Boson, and what do precision measurements of the properties of the Higgs Boson tell us about the possible properties of the superpartners?

2 LHC SUSY Searches

First, we must determine how well searches at the 7, 8 and eventually ~ 14 TeV LHC will probe the pMSSM parameter sets that we have generated. Once these constraints on the pMSSM space are known, we can determine how the properties of the lightest Higgs may differ from those of the SM in light of the (so far) null SUSY search results. Correlations between the direct search results and the properties of the Higgs then provide an answer to the first question that we posed above.

To this end we begin this step of the analysis with a short overview of the searches for the pMSSM at the 7 and 8 TeV LHC; the same overall approach will carry over to our 14 TeV

¹We note that our model sets were generated before the Higgs boson was discovered.

$m_{\tilde{L}(e)_{1,2,3}}$	100 GeV – 4 TeV
$m_{\tilde{Q}(q)_{1,2}}$	400 GeV – 4 TeV
$m_{\tilde{Q}(q)_3}$	200 GeV – 4 TeV
$ M_1 $	50 GeV – 4 TeV
$ M_2 $	100 GeV – 4 TeV
$ \mu $	100 GeV – 4 TeV
M_3	400 GeV – 4 TeV
$ A_{t,b,\tau} $	0 GeV – 4 TeV
M_A	100 GeV – 4 TeV
$\tan \beta$	1 - 60
$m_{3/2}$	1 eV – 1 TeV (\tilde{G} LSP)

Table 1: Scan ranges for the 19 (20) parameters of the pMSSM with a neutralino (gravitino) LSP. The gravitino mass is scanned with a log prior. All other parameters are scanned with flat priors, though we expect this choice to have little qualitative impact on our results based on previous studies [5, 16].

study. In general, we follow the suite of ATLAS SUSY search analyses as closely as possible employing fast Monte Carlo. These are also supplemented by several searches performed by CMS. The specific analyses applied to the neutralino model set are briefly summarized in Tables 2 and 3. We augment the standard SUSY searches by including searches for heavy stable charged particles and heavy neutral SUSY Higgs decay into $\tau^+\tau^-$ as performed by CMS [17] and measurements of the rare decay mode $B_s \rightarrow \mu^+\mu^-$ as discovered by CMS and LHCb [18]. All of these play distinct but important roles in restricting the pMSSM parameter space. Presently, we have implemented every relevant ATLAS SUSY search publicly available as of the beginning of March 2013. This list is currently being updated and expanded for future analysis. The analysis results for all three of these model sets discussed here appear in detail in our companion HE4 Snowmass White Paper on SUSY searches [13].

Very briefly stated, our procedure is as follows: We generate SUSY events for each model for all relevant (up to 85) production channels in PYTHIA 6.4.26 [19], and then pass the events through fast detector simulation using PGS 4 [20]. Both programs have been modified to, e.g., correctly deal with gravitinos, multi-body decays, hadronization of stable colored sparticles, and ATLAS b-tagging. We then scale our event rates to NLO by calculating the relevant K-factors using Prospino 2.1 [21]. The individual searches are then implemented using our customized analysis code [16], which follows the published cuts and selection criteria as closely as possible. This analysis code is validated for each of the many search regions for every analysis employing the benchmark model points provided by ATLAS (and CMS). Models are then excluded using the 95% CL_s limits as obtained by ATLAS (and CMS). For the two large model sets these analyses are performed *without* requiring the Higgs mass constraint, $m_h = 126 \pm 3$ GeV (combined experimental and theoretical errors) so that we can understand its influence on the search results. Recall that roughly $\sim 20(10)\%$ of models in the neutralino (gravitino) model set predict a Higgs mass in the above range.

Search	Reference	Neutralino	Gravitino	Low-FT
2-6 jets	ATLAS-CONF-2012-033	21.2%	17.4%	36.5%
multijets	ATLAS-CONF-2012-037	1.6%	2.1%	10.6%
1-lepton	ATLAS-CONF-2012-041	3.2%	5.3%	18.7%
HSCP	1205.0272	4.0%	17.4%	<0.1%
Disappearing Track	ATLAS-CONF-2012-111	2.6%	1.2%	<0.1%
Muon + Displaced Vertex	1210.7451	-	0.5%	-
Displaced Dilepton	1211.2472	-	1.1%	-
Gluino \rightarrow Stop/Sbottom	1207.4686	4.9%	3.5%	21.2%
Very Light Stop	ATLAS-CONF-2012-059	<0.1%	<0.1%	0.1%
Medium Stop	ATLAS-CONF-2012-071	0.3%	5.1%	2.1%
Heavy Stop (0l)	1208.1447	3.7%	3.0%	17.0%
Heavy Stop (1l)	1208.2590	2.0%	2.2%	12.6%
GMSB Direct Stop	1204.6736	<0.1%	<0.1%	0.7%
Direct Sbottom	ATLAS-CONF-2012-106	2.5%	2.3%	5.1%
3 leptons	ATLAS-CONF-2012-108	1.1%	6.1%	17.6%
1-2 leptons	1208.4688	4.1%	8.2%	21.0%
Direct slepton/gaugino (2l)	1208.2884	0.1%	1.2%	0.8%
Direct gaugino (3l)	1208.3144	0.4%	5.4%	7.5%
4 leptons	1210.4457	0.7%	6.3%	14.8%
1 lepton + many jets	ATLAS-CONF-2012-140	1.3%	2.0%	11.7%
1 lepton + γ	ATLAS-CONF-2012-144	<0.1%	1.6%	<0.1%
$\gamma + b$	1211.1167	<0.1%	2.3%	<0.1%
$\gamma\gamma + \text{MET}$	1209.0753	<0.1%	5.4%	<0.1%
$B_s \rightarrow \mu\mu$	1211.2674	0.8%	3.1%	*
$A/H \rightarrow \tau\tau$	CMS-PAS-HIG-12-050	1.6%	<0.1%	*

Table 2: 7 TeV LHC searches included in the present analysis and the corresponding fraction of the neutralino, gravitino and low-FT pMSSM model sets excluded by each search. Note that in the case of the last two entries the experimental constraints have already been included in the model generation process for the low-FT model set and therefore are not shown here.

Search	Reference	Neutralino	Gravitino	Low-FT
2-6 jets	ATLAS-CONF-2012-109	26.7%	21.6%	44.9%
multijets	ATLAS-CONF-2012-103	3.3%	3.8%	20.9%
1-lepton	ATLAS-CONF-2012-104	3.3%	6.0%	20.9%
SS dileptons	ATLAS-CONF-2012-105	4.9%	12.4%	35.5%
Medium Stop (2l)	ATLAS-CONF-2012-167	0.6%	8.1%	4.9%
Medium/Heavy Stop (1l)	ATLAS-CONF-2012-166	3.8%	4.5%	21.0%
Direct Sbottom (2b)	ATLAS-CONF-2012-165	6.2%	5.1%	12.1%
3rd Generation Squarks (3b)	ATLAS-CONF-2012-145	10.8%	9.9%	40.8%
3rd Generation Squarks (3l)	ATLAS-CONF-2012-151	1.9%	9.2%	26.5%
3 leptons	ATLAS-CONF-2012-154	1.4%	8.8%	32.3%
4 leptons	ATLAS-CONF-2012-153	3.0%	13.2%	46.9%
Z + jets + MET	ATLAS-CONF-2012-152	0.3%	1.4%	6.8%

Table 3: Same as in the previous table but now for the 8 TeV ATLAS MET-based SUSY searches. Note that when all the above searches in both Tables are combined for the neutralino (gravitino, low-FT) model set we find that ~ 37 (52, 70)% of these models are currently excluded by the LHC.

While there is some variation amongst the individual searches themselves, we find that, once combined, the total fraction of our models surviving the set of all LHC searches is to an excellent approximation *independent* of whether or not the Higgs mass constraint has been applied. Conversely, the $\sim 20(10)\%$ fraction of neutralino (gravitino) models predicting the correct Higgs mass is also found to be approximately independent of whether the SUSY searches have been applied. This result is very powerful and demonstrates the approximate decoupling of direct SUSY search results from the discovery of the Higgs boson, allowing us, in general, to continue examining the properties and signatures of the entire neutralino and gravitino model samples with some reasonable validity. Of course, for this study, in which we examine the properties of the Higgs boson itself, we restrict our analysis to the subsets of the neutralino and gravitino model sets which predict $m_h = 126 \pm 3$ GeV. No additional requirements on the Higgs mass are necessary for the low-FT set, since in this case the Higgs mass constraint is imposed during model generation.

3 Determination of Higgs Properties in the pMSSM

The next part of this project is to use the measured properties of the Higgs to directly constrain the pMSSM parameter space. To do this we determine the extent to which the couplings of the light CP-even Higgs boson in the pMSSM differ from the Standard Model expectations, then compare these results to current and future experimental determinations of the couplings. We make several comparisons corresponding to the anticipated evolution of our knowledge about the allowed values of the couplings: (*i*) limits from current data [22], (*ii*) limits that are expected to be attainable at the 14 TeV LHC with an integrated luminosity of

0.3(3) ab^{-1} [23], and finally (iii) projected limits from the ILC [24]. To this end we employ the latest version of HDECAY 5.11 to calculate these coupling ratios in the analysis that follows. Note that since the full SUSY loop corrections for the $h \rightarrow WW$ and $h \rightarrow ZZ$ partial widths are not yet incorporated in HDECAY, we unfortunately can not employ these very important modes to constrain our model sample.

We will follow the standard approach here and define the signal strength for production of a final state produced from the decay $h \rightarrow X$ via a given production channel (e.g. $gg, VBF \rightarrow h$), normalized to the corresponding SM value as

$$\mu_{gg,VBF}(X) = \frac{\sigma(gg, VV \rightarrow h) B(h \rightarrow X)}{SM}. \quad (1)$$

For final states X which do not involve the top quark, we can also define the ratio of the squares of the various effective couplings to their corresponding SM values by simply forming the ratios of the relevant partial decay widths,

$$r_X = \frac{\Gamma(h \rightarrow X)}{SM}, \quad (2)$$

for the final states $X = ZZ, W^+W^-, \bar{b}b, \bar{c}c, \tau^+\tau^-, gg, \gamma\gamma, \gamma Z$; the case of the $ht\bar{t}$ coupling must be handled separately and can only be directly accessed via associated production. We are, of course, also interested in the branching fraction for the invisible Higgs decays into, e.g., the lightest neutralino, producing a final state which is pure MET². Searches for invisible decays into these LSPs are very interesting because of their potential to place significant constraints on the SUSY parameter space, particularly when results from ILC500 are employed.

To get an initial idea of the distribution of Higgs properties in the various model sets it is instructive to look at a few examples. Consider Fig. 1, which shows the distribution of the $h \rightarrow \gamma\gamma$ signal strength for both the gg -fusion and vector boson fusion production channels in the neutralino LSP model subset with $m_h = 126 \pm 3$ GeV, along with the effect of current and future ATLAS searches on this distribution [13]. Other than the obvious fact that these distributions peak near unity but have long tails, the most important thing to notice is that the *shape* of these distributions (up to statistical fluctuations) is essentially unaffected by the ATLAS direct SUSY searches. Furthermore, the shape of the $r_{total} = \Gamma(h \rightarrow All)/SM$ distribution for the neutralino set also shows that this shape invariance is maintained for the other observables. We therefore see that SUSY searches and Higgs boson properties are to a very good approximation orthogonal. As we will show below, the other final states exhibit a similar behavior, answering the first question posed in the abstract - future null searches at the LHC will, to a good approximation, not affect the range of values that we might expect for the Higgs couplings.

We now turn our attention to the predicted distributions for the values of the various partial width distributions, r_X , in each model set, and the effect of future LHC searches

²Decays to other sparticles are kinematically forbidden as a result of the LEP limits on charged particles; neutral winos and Higgsinos as well as sneutrinos are required to have a charged partner with a similar mass, preventing them from being decay products of a ~ 126 GeV Higgs.

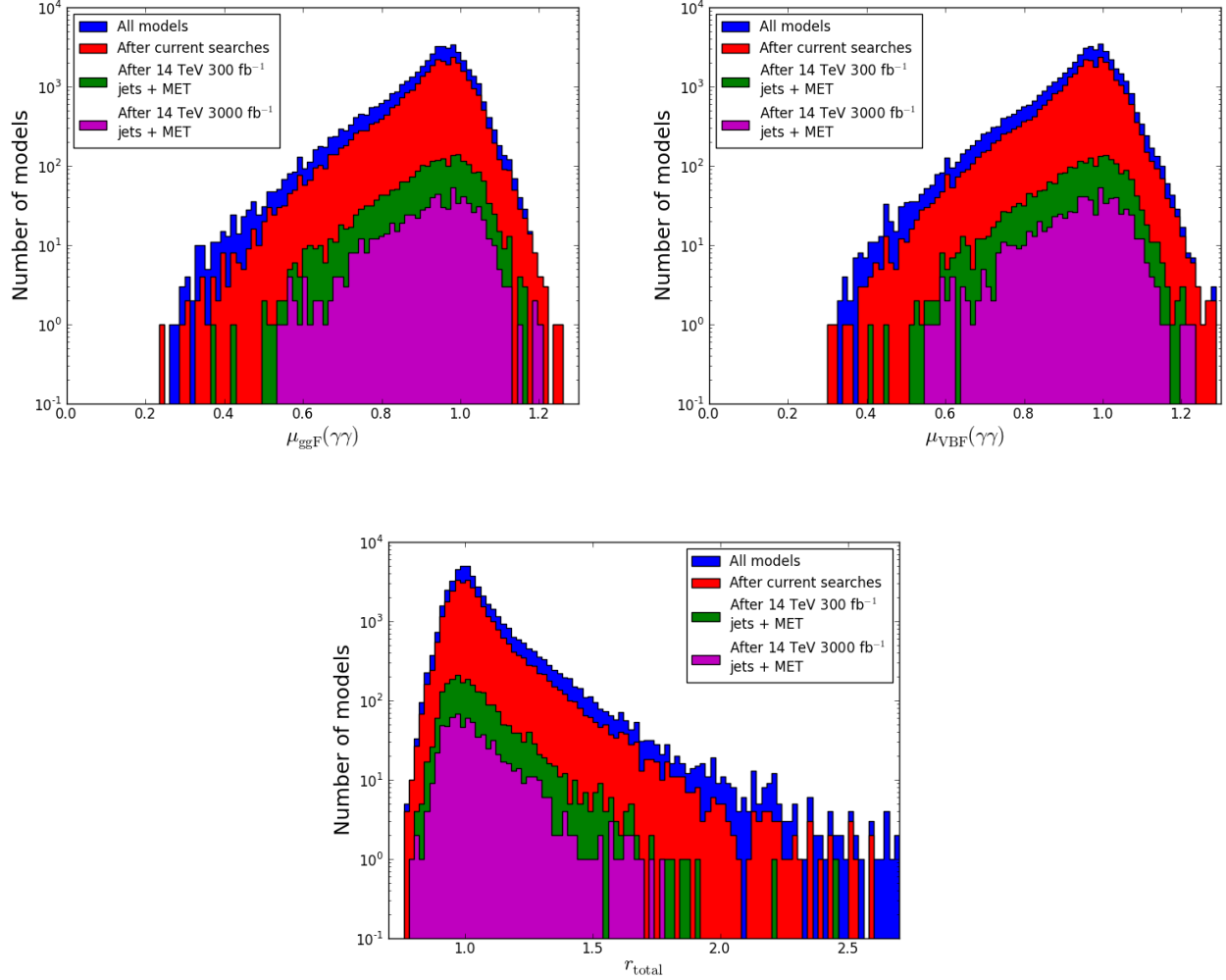


Figure 1: Histograms of signal strengths for $h \rightarrow \gamma\gamma$ in the gg -fusion (top left) and vector boson fusion (top right) channels for the subset of neutralino models that predict $m_h = 126 \pm 3$ GeV. The blue (red) histogram represents models before any ATLAS searches are applied (after the 7 and 8 TeV SUSY searches) while the green (purple) histograms show models that are expected to survive the zero-lepton jets plus MET search at 14 TeV, assuming a luminosity of 300 (3000) fb^{-1} . The ratio r_{total} for the total h width is analogously shown in the bottom panel.

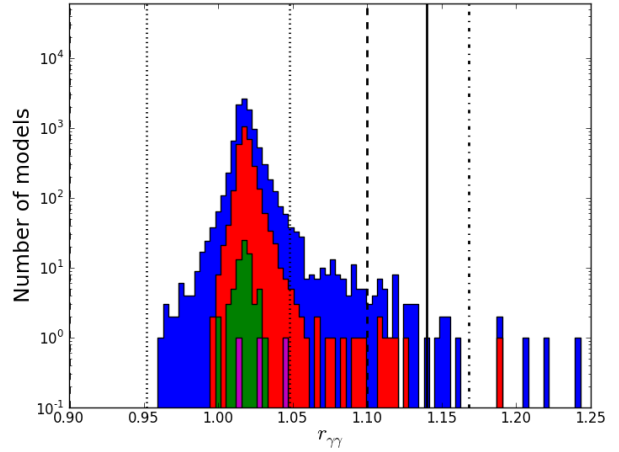
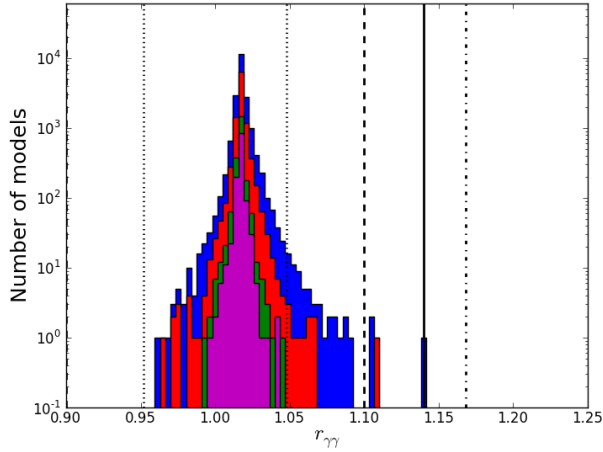
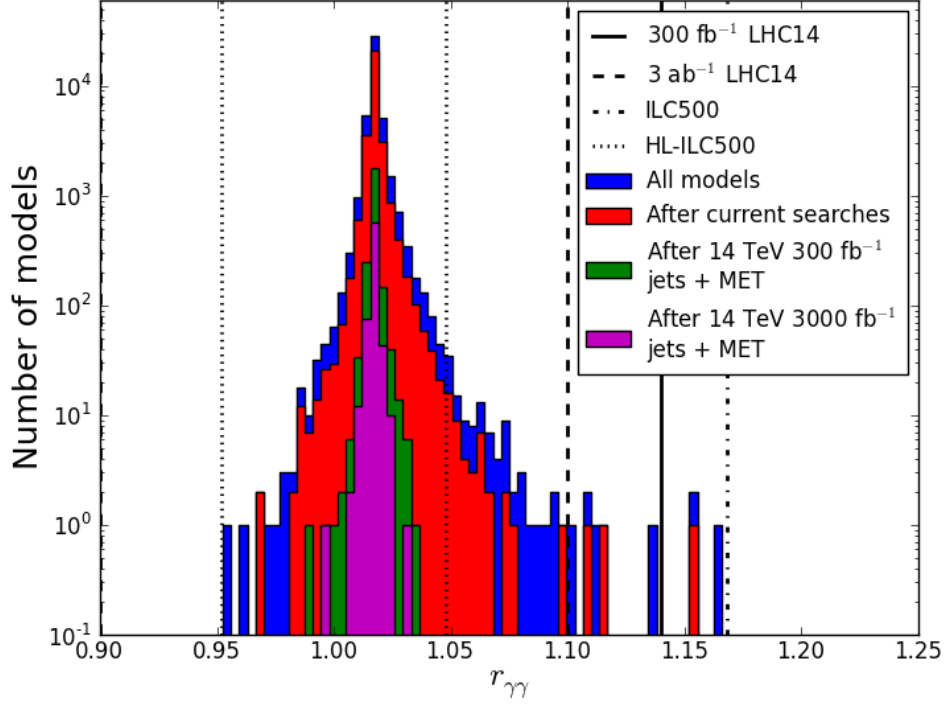


Figure 2: Histograms of the partial width ratio for $h \rightarrow \gamma\gamma$ for the subset of neutralino (top), gravitino (lower left) and low-FT models (lower right) that predict $m_h = 126 \pm 3$ GeV. The blue (red) histogram represents models before any ATLAS searches are applied (after the 7 and 8 TeV SUSY searches) while the green (purple) histograms show models that are expected to survive the zero-lepton jets plus MET search at 14 TeV, assuming a luminosity of 300 (3000) fb^{-1} . The vertical lines show the expected future limits on $r_{\gamma\gamma}$, and are discussed in Section 4.

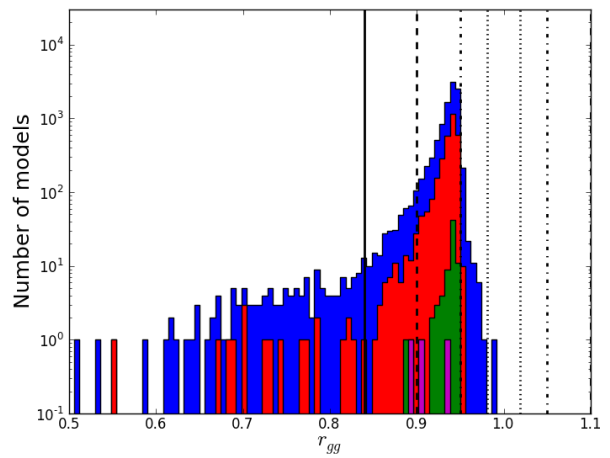
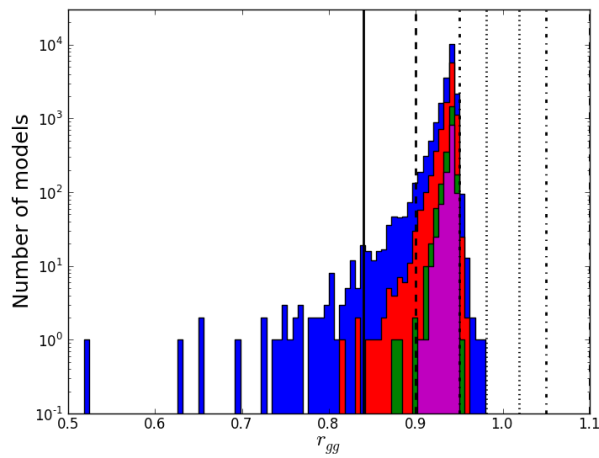
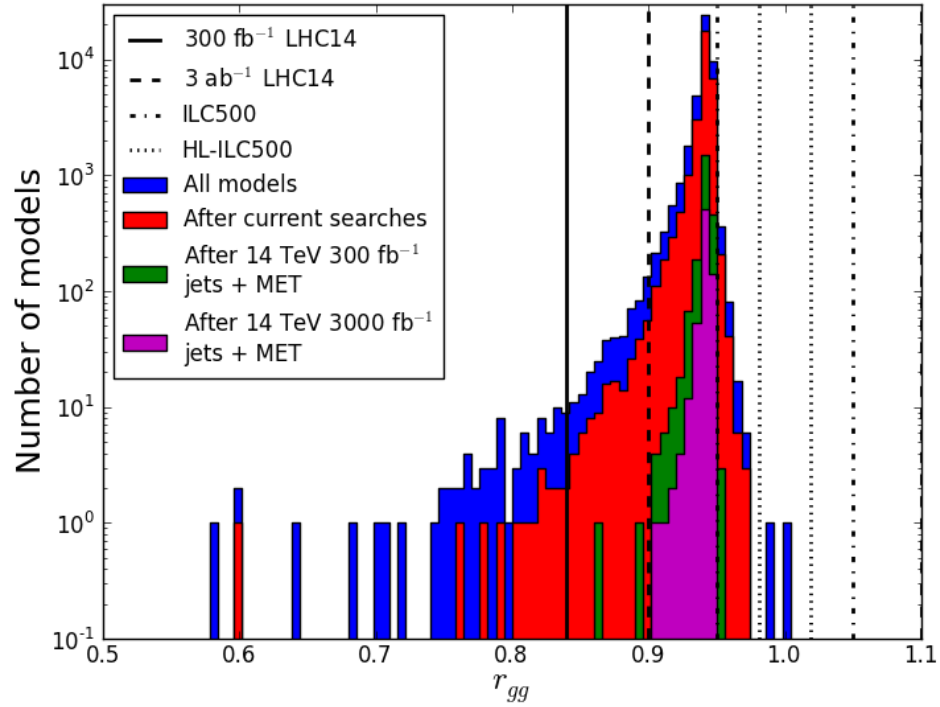


Figure 3: Same as the previous Figure but now for $h \rightarrow gg$.

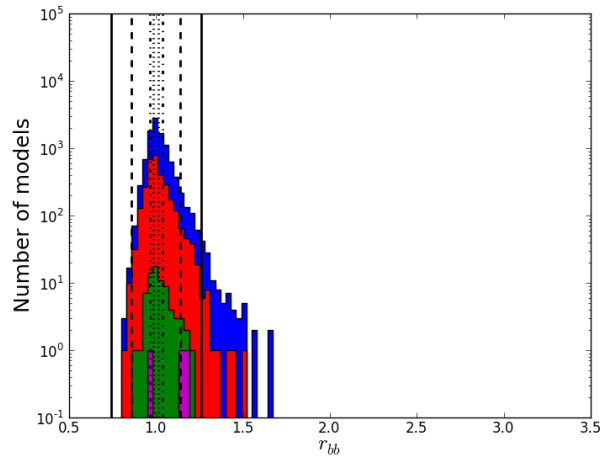
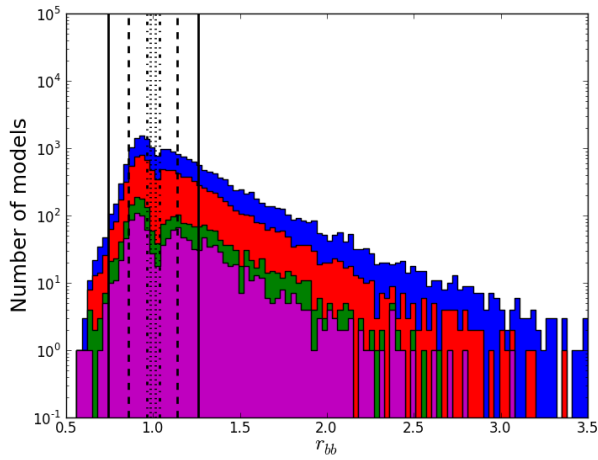
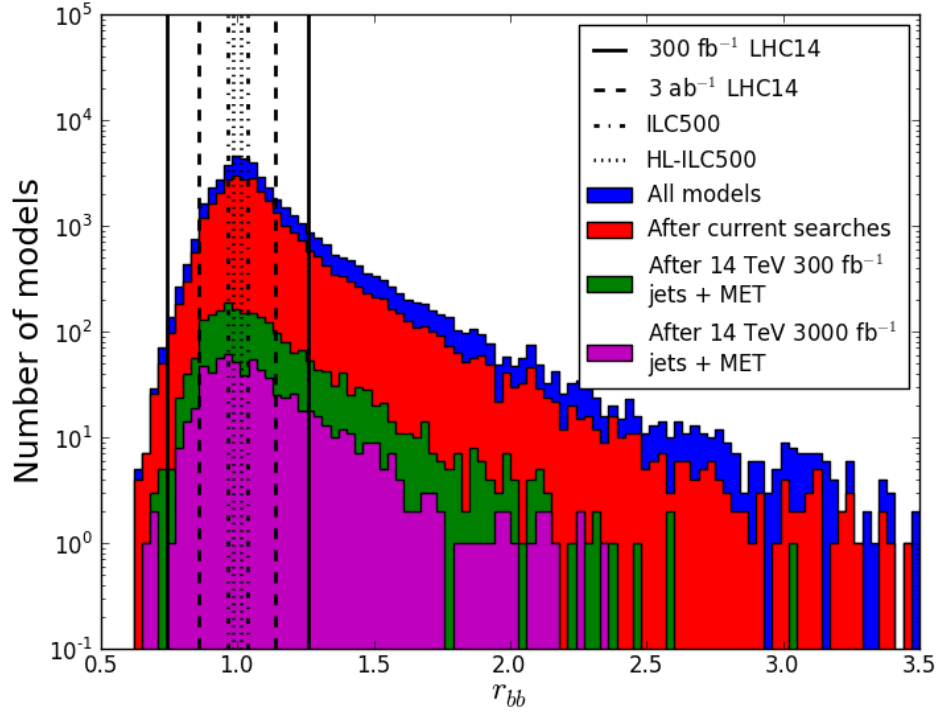


Figure 4: Same as in Figure 2 but now for $h \rightarrow b\bar{b}$.

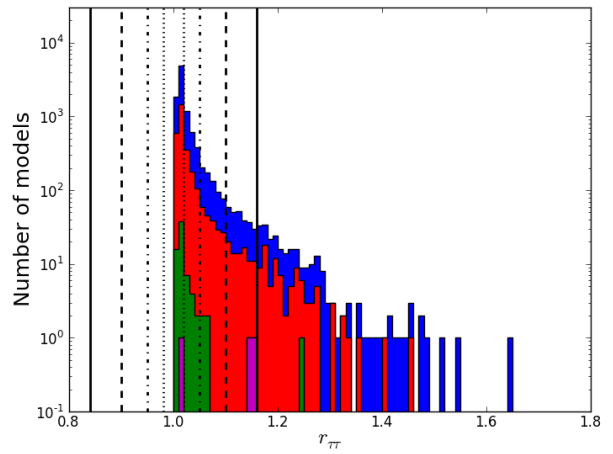
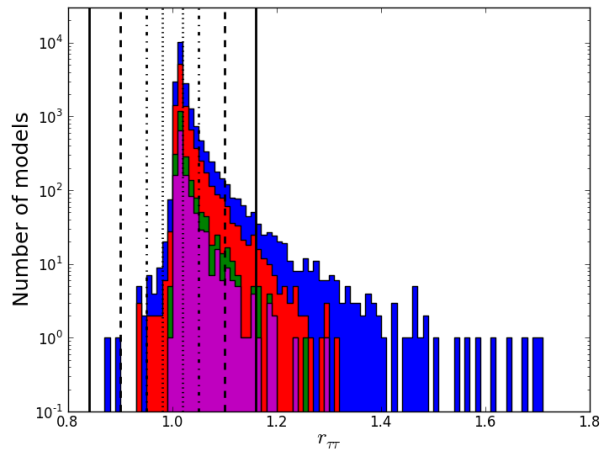
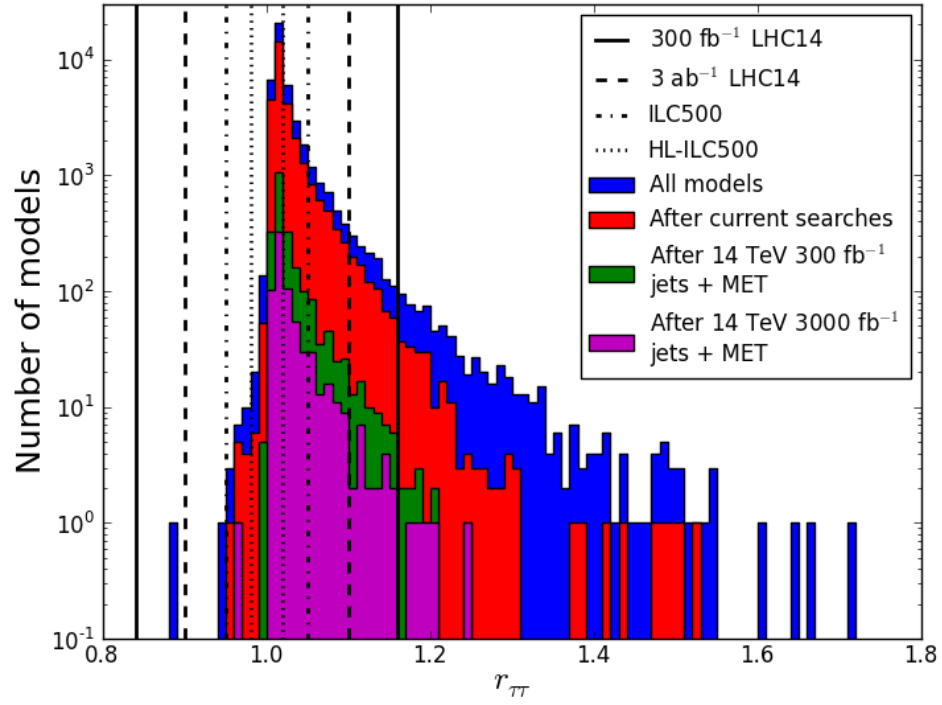


Figure 5: Same as in Figure 2 but now for $h \rightarrow \tau^+\tau^-$.

on these distributions. We will return to these distributions in our subsequent analysis to understand the effects of future Higgs coupling measurements.

Figure 2 shows the histogram of values for the SM-normalized partial decay width $r_{\gamma\gamma}$ for the three different model sets. The vertical lines appearing in these plots are discussed in the next section. Qualitatively we see that the effect of LHC searches on the $r_{\gamma\gamma}$ distributions is to decrease the normalization while preserving the shapes of the distributions; deviations from this behavior are seen mainly in the tails of the distributions, where the statistics are low. The different responses of each model set to the direct LHC SUSY searches can be seen by observing the widely differing impacts of the searches on the distribution areas. Interestingly, the shape of the distribution of $r_{\gamma\gamma}$ in the neutralino model set is very different from the corresponding distribution of diphoton signal strengths shown in Figure 1, a difference which results mainly from large corrections to the $h \rightarrow b\bar{b}$ partial width (which will be discussed below), and therefore to the total width. These corrections alter the diphoton branching fraction, and therefore the signal strength, for a given value of $r_{\gamma\gamma}$. Note also that the distributions of $r_{\gamma\gamma}$ in the neutralino and gravitino model sets are rather similar and somewhat distinct from the corresponding distribution in the low-FT model set, which exhibits a somewhat broader range of values for $r_{\gamma\gamma}$ despite lower statistics. The larger spread in the low-FT distribution arises from the mandatory presence of light charginos, stops, and (in many cases) sbottoms, typically resulting in larger SUSY corrections to the effective $h\gamma\gamma$ coupling than in the neutralino and gravitino model sets, in which charged sparticles are not required to be relatively light. Finally, note that in all three model sets the value of $r_{\gamma\gamma}$ peaks at the same value, slightly above unity. We will see below that this shift is reasonably correlated with an opposite shift in the peak of the r_{gg} distribution, and that both offsets result from the large stop mixing that is necessary to obtain the correct Higgs mass.

Figure 3 displays the corresponding histograms for the values of r_{gg} , again showing the distribution for each model set. Once again, the neutralino and gravitino distributions are quite similar while the low-FT distribution is different as a result of distinct requirements on the sparticle spectra. As shown in, *e.g.*, [25], the large Higgs mass in the pMSSM generally requires large stop mixing, which results in a small ($\sim 7\%$) but important reduction in the $h \rightarrow gg$ partial width and a simultaneous enhancement in the $h \rightarrow \gamma\gamma$ partial width. If the stop sector is totally responsible for this shift (which is a reasonable approximation in many cases), then the shift in r_{gg} at the amplitude level is ~ 3 times larger than the corresponding shift in $r_{\gamma\gamma}$, with the two shifts having opposite signs. As a result of this effect, nearly all of our models predict r_{gg} to be below unity, an observation which will figure prominently in our subsequent discussion of future experimental constraints on the Higgs couplings. Interestingly, we also see that the tails of the r_{gg} distribution, though present, are not very large. They are slightly larger in the low-FT r_{gg} distribution, since the relevant corrections tend to be larger as a result of the bias towards light stops in the low-FT model set.

Figure 4 shows the results for the ratio r_{bb} for the three different model sets, with the neutralino and gravitino distributions again differing somewhat from the low-FT distribution. Small differences between the neutralino and gravitino distributions arise from, *e.g.*, the fact

that lighter stops can appear in the gravitino set, since the requirement for the stop to be heavier than the LSP is trivially satisfied by $m_{LSP} \sim 0$ in most of the gravitino LSP models. For each model set we see the now familiar pattern in which the LHC searches do not significantly alter the shapes of the partial width distributions. Unlike the previous cases, however, we now see that r_{bb} may deviate from unity by an $O(1)$ factor. These deviations result from large sbottom mixings that can make $O(1)$ changes in the $hb\bar{b}$ couplings through non-decoupling (mostly gluino) loop effects. These loop effects are driven by the size of the off-diagonal piece of the sbottom mass matrix $m_b(A_b - \mu \tan \beta)$, which is enhanced for large values of $\tan \beta$. While the tail mostly extends to larger values of r_{bb} , we see that models also exist with r_{bb} significantly below unity. Since the $b\bar{b}$ mode dominates the Higgs width, this same effect also explains the large spread in the distribution of r_{total} , shown for the neutralino model set in Fig. 1 and described above. In our neutralino and gravitino parameter scans, $|A_b|$ and $|\mu|$ are typically of a similar size while $\tan \beta$ has typical values that are $O(10)$, so it is the $\mu \tan \beta$ term in the off-diagonal piece that dominates. However, in the low-FT set this is no longer true as $|\mu|$ is now forced to be relatively small. Thus in the low-FT case we do not expect the range of values for r_{bb} to be as large as it is in the neutralino and gravitino sets; this is exactly what we see in Fig. 4.

Figure 5 shows the analogous results for the ratio $r_{\tau\tau}$ for the three different model sets. Here we again see that the shapes of the $r_{\tau\tau}$ histograms are not significantly altered by the ATLAS SUSY searches at this level of statistics. We also see that the peak occurs at a value slightly greater than unity (by $\sim 2\%$) with a significant tail extending to larger values. This is not surprising since there are also non-decoupling effects in the corrections to the $h\tau\tau$ vertex, although they occur via electroweakino loops and are proportional to the τ mass. This implies that the effect of these non-decoupling terms should be relatively small when compared with their effect in the case of r_{bb} , and that is indeed what we observe. Again, since this non-decoupling occurs via the off-diagonal $m_\tau(A_\tau - \mu \tan \beta)$ term in the stau mass matrix, these effects should be somewhat suppressed in the low-FT model set in comparison to the other model sets, and this is demonstrated in Figure 5.

Figure 6 shows the dependence of r_{bb} on the lighter sbottom mass for the neutralino LSP models as the effects of the direct LHC SUSY searches are imposed. Clearly, measuring a value of this ratio near unity will not impose a constraint on the sbottom mass, regardless of the precision of the measurement. On the other hand, very large deviations of this ratio from unity are seen to require a relatively light sbottom mass, meaning that null SUSY search results should be able to reduce the allowed range for r_{bb} . However, the non-decoupling nature of the corrections means that values of r_{bb} above 2 remain allowed even after the 14 TeV jets + MET search is included; excluding $O(1)$ deviations from $r_{bb} = 1$ (which can occur for sbottoms as heavy as 2.5 TeV) through SUSY searches is clearly beyond the capability of the LHC. The large sbottom mass reach necessary to constrain r_{bb} significantly explains our earlier observation that its distribution is roughly independent of applying the LHC searches, although we see now that the 14 TeV searches do begin to have an impact at the edges of the r_{bb} distribution. Although we do not show them here, the corresponding results for the gravitino set are found to be qualitatively similar to those for the neutralino set, although

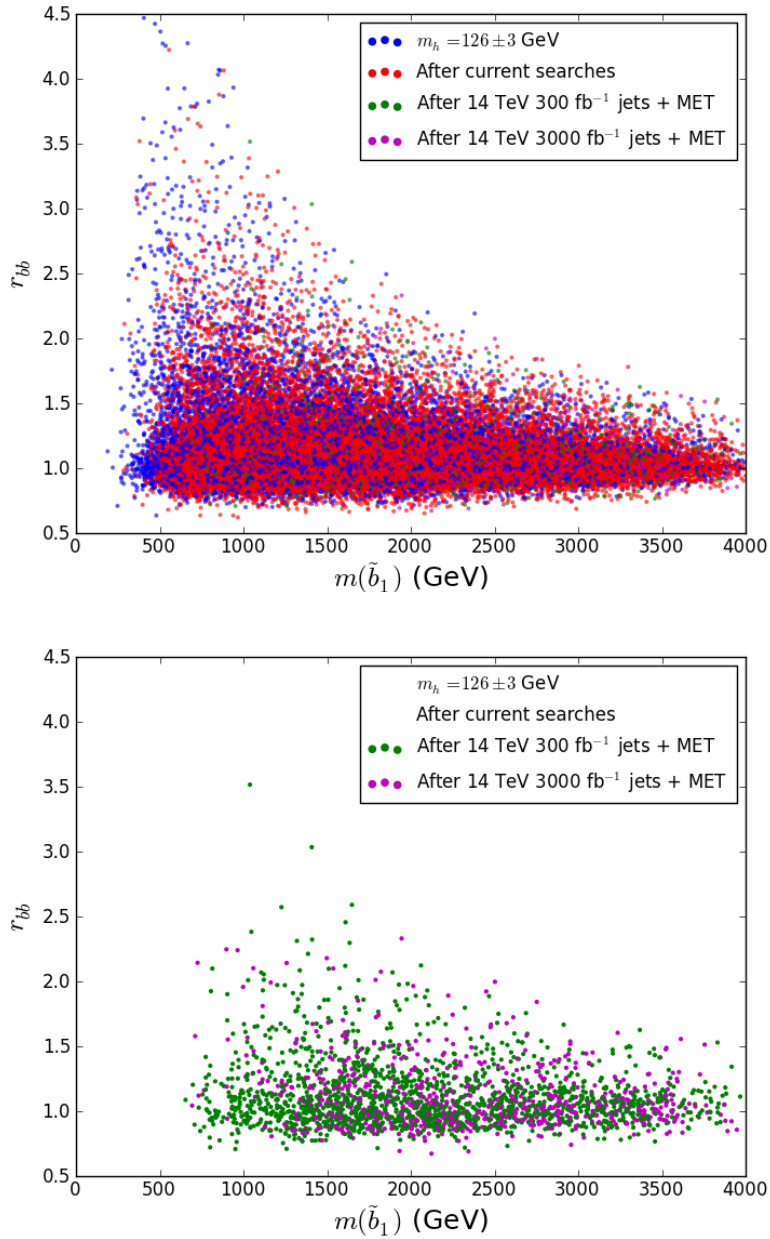


Figure 6: Values of r_{bb} as a function of the lightest sbottom mass for the neutralino model set showing the influence of the ATLAS SUSY searches. The lower panel shows those models surviving the zero lepton, jets plus MET search at 14 TeV.

they differ in detail due to the contrasting reach of direct sparticle searches in these two sets. Figure 7 shows the analogous result for the low-FT model set. The essential reason for the shapes in this figure has already been discussed above; since in the low-FT set $|\mu|$ needs to be relatively small, the size of the off-diagonal element in the sbottom mass matrix is decreased, and the corrections to r_{bb} become significantly smaller.

The top panel in Fig. 8 shows the Higgs invisible branching fraction, $B(h \rightarrow \chi\chi)$, as a function of the LSP mass for the few neutralino LSP models for which this is kinematically allowed and how they respond to the direct SUSY searches at the LHC. Note that all of these models have $B(h \rightarrow \chi\chi) < 0.5$, meaning that they remain unconstrained by current LHC Higgs data. However, we note that all of these models *will* eventually be excluded (or discovered) by sparticle searches as well as by searches for Higgs \rightarrow invisible at the 14 TeV LHC and/or ILC500. The lower left panel shows the corresponding results for the gravitino set; here we see that for these models a much smaller branching fraction is obtained. Of course for these gravitino models the lightest neutralinos will only produce an invisible final state if they escape the detector before decaying; neutralinos with $c\tau \lesssim 1\text{m}$ will have visible decays, generally producing a (possibly displaced) diphoton + MET signature, where the diphotons would of course fail to reconstruct the Higgs mass. However, the stability of the neutralino tends to be unimportant, since (with the possible exception of the model with the lightest neutralino) the $h \rightarrow \chi\chi$ branching fractions seen here are far too small to be accessible at the 14 TeV LHC. The bottom right panel shows the same distribution, now for the low-FT model set. Here we see that the additional constraints imposed on the pMSSM spectrum yield many light LSPs which are mainly bino-Higgsino admixtures, a sizeable fraction of which pair-annihilate via the Higgs funnel. In all cases, however, the invisible branching fraction is found to be below $\sim 20\%$, which will barely be accessible at the 14 TeV LHC. While many of these models are now excluded by LHC SUSY searches, the remainder would be excluded by the 14 TeV jets plus MET search.

Although we do not include the ratio r_{tt} directly in our analysis, the predicted values of this quantity found in the various model sets are of some interest. Figure 9 displays the ratio r_{tt} for the various model sets as a function of the lightest stop mass, where we here have defined r_{tt} as the ratio of the square of the effective $ht\bar{t}$ coupling to its SM value, employing the approximation provided in [26]. Here we see that, *e.g.*, in the case of the low-FT set, significant deviations of this ratio away from unity (*e.g.*, $r_{tt} > 2$, say) require stop masses below $\simeq 650$ GeV. However, as in the case of the ratio r_{bb} discussed above, a measurement of r_{tt} near unity will not exclude any particular range of stop masses in this model set. Note that both the neutralino and gravitino model sets, for which similar results are obtained, can easily produce significant departures of r_{tt} from unity even with relatively heavy stop masses. For these model sets, values of r_{tt} as large as 2 can be achieved for lightest stop masses up to ~ 1.6 TeV. This wider range of allowed values in the neutralino and gravitino model sets should not be too surprising since the stop mass matrix and the resulting physical mass spectrum are not constrained in these models by the additional requirements placed on the low-FT set.

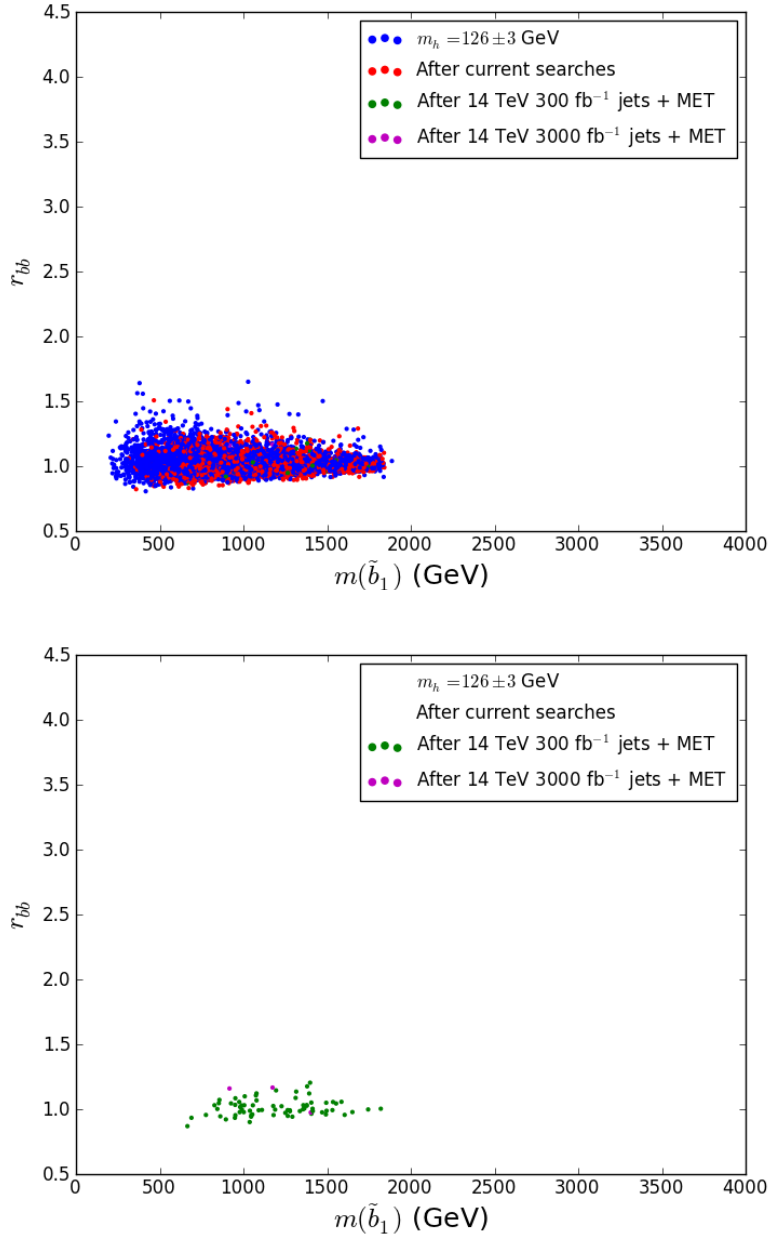


Figure 7: Same as the previous Figure but now for the low-FT model set.

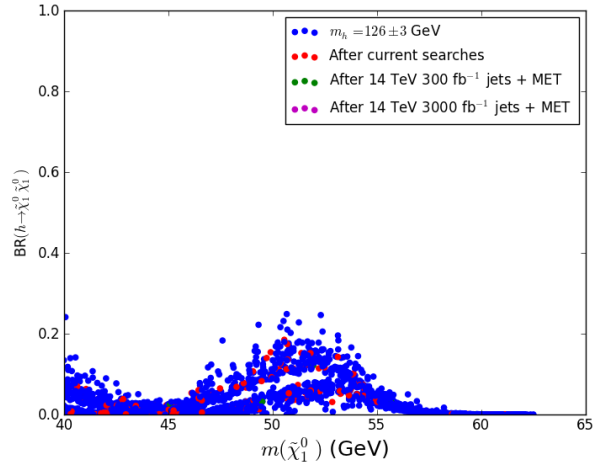
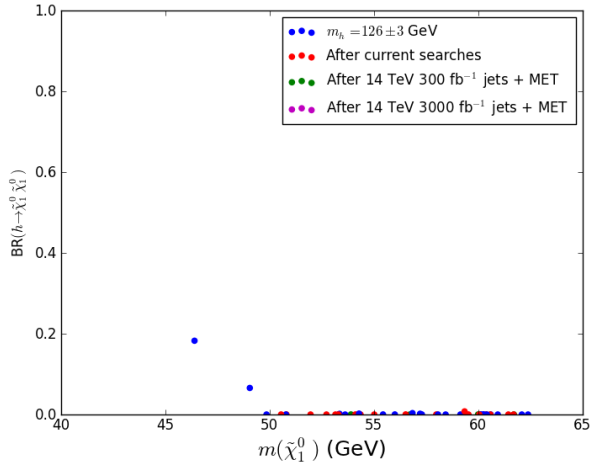
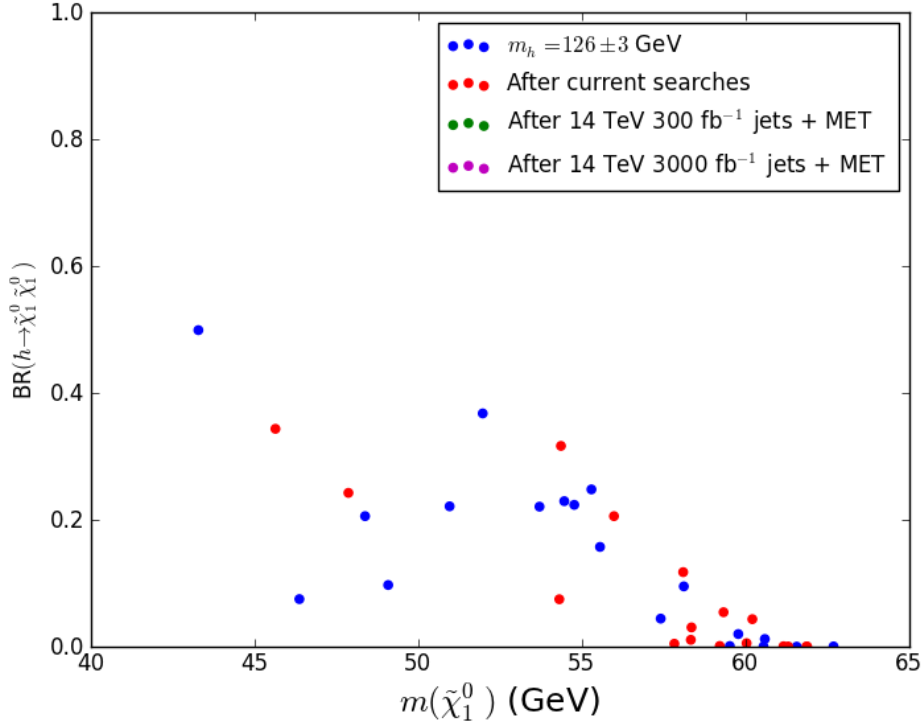


Figure 8: (Top) Branching fraction for invisible Higgs decays ($h \rightarrow \chi_1^0 \chi_1^0$) for neutralino LSP models with the correct Higgs mass. The points are color-coded according to their response to the LHC SUSY searches. The analogous results for the gravitino (bottom left) and low-FT (bottom right) model sets are also shown.

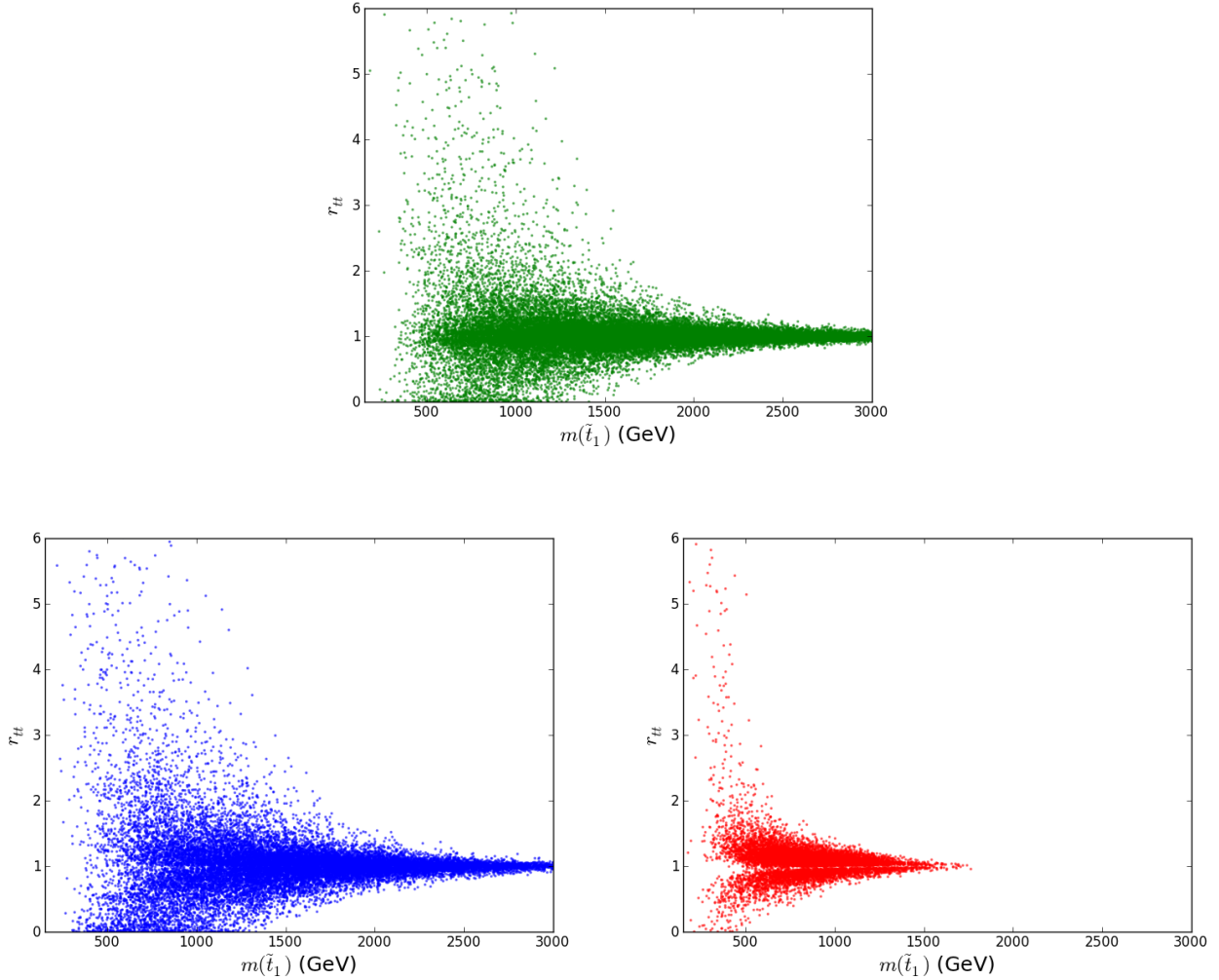


Figure 9: The predicted values of the ratio r_{tt} (the squared $ht\bar{t}$ coupling normalized to its SM value) for the various pMSSM models as a function of the lightest stop mass. The top (lower left, lower right) panel shows the results for the neutralino (gravitino, low-ft) model set.

4 Analysis and Results

Now that we have assembled the necessary pieces for our analysis, we can ask how the measurements of the various Higgs couplings at the LHC and ILC will constrain the pMSSM parameter space, and how these constraints compare with those from direct SUSY searches. In what follows, we will make use of the numerical results for current and future Higgs coupling measurements as presented in Refs. [22–24]. Note that in the results quoted below, in taking allowed ranges for the ratios of pMSSM to SM Higgs couplings, we will ignore potentially significant theoretical uncertainties (as important higher order corrections have yet to be calculated) which may be quite important given the claimed level of precision for future LHC and ILC coupling measurements. We remind the reader to keep this important issue in mind when interpreting our results; our results should thus be treated as indicative only. Clearly more theoretical work will be necessary before (sub-)percent-level measurements are truly meaningful.

We first note that the current LHC data does not significantly constrain the pMSSM parameter space, since the precision of the Higgs coupling measurements is still rather low in comparison to the deviations that we expect in our pMSSM model sets. Once 14 TeV LHC and ILC data is available, this will no longer be the case. Even more importantly, we note that in order to obtain the results we show below, *we have assumed* that the central values of the couplings measured at both the LHC and ILC will coincide *exactly* with the SM values, and furthermore ignore the theoretical uncertainties associated with the pMSSM predictions themselves (relative to those of the SM at the very least). As the reader will see from the discussion and the Tables that follow, the observation of central values differing from the SM prediction (even within the expected ranges) will most certainly exclude a different fraction of our models. This is particularly true for both the loop-sensitive ratios r_{gg} and $r_{\gamma\gamma}$, for which the predicted deviations from the SM values in the pMSSM are essentially all in one direction. Of course our qualitative results, which indicate that precise Higgs coupling measurements (when properly understood) have significant sensitivity to our pMSSM models, do *not* depend on the actual central values that will be observed for these couplings.

Assuming that the measured central value of each parameter is equal to the SM prediction, we return to Figs. 2, 3, 4 and 5 and now concentrate on the vertical lines, which show the expected sensitivity at future experiments. These show the regions of the various r_X for the the three model sets which will be allowed or excluded at the 95% CL by Higgs coupling measurements at the LHC and HL-LHC [23], the 500 GeV ILC (ILC500) and the ILC500 with a luminosity upgrade [24], here denoted as HL-ILC500. Of course, it is important to note that we can always slide these ‘allowed’ regions around to estimate the implications of other possible central value measurements. However, the key result here is that, regardless of what central values are actually observed, *indirect Higgs coupling measurements will likely result in the exclusion (or discovery) of pMSSM models which are not accessible to direct SUSY searches at the LHC*. An important caveat to this, of course, is that we need to include (many) more 14 TeV SUSY searches before this result can be shown to be truly robust. However, we know from our 7 and 8 TeV studies that the zero-lepton, jets plus MET search

will almost certainly be the most powerful search at 14 TeV, as least for the neutralino and low-FT model sets, and so this qualitative conclusion is unlikely to change.³ This result is seen to hold for all of the model sets.

Taking these results at face value (but remembering the above caveats), we can extract some relevant numbers directly from these Figures. The first question we can now address is what fraction of the presently allowed (*i.e.*, those passing the 7 and 8 TeV ATLAS analyses and predicting $m_h = 126 \pm 3$ GeV) pMSSM models will be indirectly excluded by future measurements of the Higgs couplings by the LHC and ILC for the three different model sets? The second question is how will these results be modified by the 14 TeV LHC SUSY searches? The answers to these questions for both the 14 TeV LHC and the ILC can be seen in the set of Tables 4, 5 and 6. In these Tables we see a number of important results: (*i*) at the LHC, constraining the $hb\bar{b}$ coupling yields the strongest limits on the allowed pMSSM parameter space. This could also be true at the ILC depending on the observed central values for the measured couplings. However, *if* we assume that the central values exactly correspond to the SM values, we see that the ILC determination of the hgg coupling does much of the damage to the remaining parameter pMSSM space. The reason for this is clear: since r_{gg} is forced to be less than unity by the stop mixing required to produce the correct value of the Higgs mass, measuring $r_{gg} = 1$ with a very small error will exclude essentially all of the model sets! If, on the other hand, the central value were measured to be only $\sim 2 - 3\%$ *below* unity, a much smaller percentage of models would then be excluded. For example, if the central value of r_{gg} were measured to be 0.97 with the same errors, then we would find that this measurement would only exclude 2.7% of the neutralino LSP models at ILC500 and that $hb\bar{b}$ would remain the dominant constraint on this model set in this case. We therefore see that in this specific case our results are sensitive to our assumption that the measured central values will agree with the predicted SM values. In any case, (*ii*) we see that both the LHC and ILC will provide very powerful constraints on the pMSSM model space and have the potential to exclude models that would otherwise remain allowed even after the SUSY searches are performed. In particular, the precision available on Higgs couplings at the ILC will deeply probe the pMSSM parameter space.

Tables 4-6 also show that (*iii*) although the general shapes of the r_X distributions are somewhat similar they differ in detail in such a way that the pMSSM model sets will respond distinctly to the various indirect Higgs coupling measurement constraints. Of course the ILC500 is extremely powerful in all cases. The last thing we notice is (*iv*) that the entries in the Tables do not vary greatly as we include more results from future SUSY searches. This is not surprising; in the limit that the shapes of the r_X distributions are completely unaffected by the SUSY search results, the Table entries should be independent of which LHC searches have been applied. The limited size of our model samples and the small changes in the r_X distribution shapes account for the observed variations.

³We note in our companion White Paper [13] that the 14 TeV jets+MET search has an impact on the gravitino LSP model set which is diminished, but still significant, compared with its impact on the neutralino LSP model set.

Channel	300 fb ⁻¹ LHC	3 ab ⁻¹ LHC	500 GeV ILC	HL 500 GeV ILC
$b\bar{b}$	16.4 (27.5, 0.5)	32.4 (48.5, 5.5)	77.4 (89.0, 49.0)	90.5 (95.8, 77.4)
$\tau\tau$	0.7 (0.7, 3.0)	3.1 (2.7, 5.8)	11.6 (9.7, 12.3)	36.8 (34.2, 32.8)
$g\bar{g}$	0.05 (0.03, 0.6)	0.6 (0.6, 3.1)	99.1 (99.7, 99.7)	100.0 (100.0, 100.0)
$\gamma\gamma$	0.03 (0.06, 0.03)	0.04 (0.07, 0.2)	0.03 (0.06, 0.03)	0.2 (0.15, 0.78)
Invisible	— (—, —)	— (—, —)	0.03 (0.01, 6.50)	0.04 (0.01, 7.8)
All	16.9 (27.9, 3.9)	33.9 (49.6, 11.3)	99.7 (99.96, 99.94)	100.0 (100.0, 100.0)

Table 4: The fraction in percent of neutralino (gravitino, low-FT) models with the correct Higgs mass remaining after the current 7 and 8 TeV LHC searches that are expected to be excluded by future Higgs coupling measurements, *assuming* that the SM values for these couplings are obtained. Blank entries indicate values below 0.01%.

Channel	300 fb ⁻¹ LHC	3 ab ⁻¹ LHC	500 GeV ILC	HL 500 GeV ILC
$b\bar{b}$	20.5 (31.1, 0)	39.4 (52.8, 6.8)	82.7 (92.9, 51.4)	93.1 (97.6, 77.0)
$\tau\tau$	0.5 (0.6, 1.4)	3.2 (2.5, 4.1)	12.8 (9.4, 9.5)	38.8 (32.2, 27.0)
$g\bar{g}$	0 (0, 0)	0.09 (0.2, 2.7)	99.9 (99.95, 100.0)	100.0 (100.0, 100.0)
$\gamma\gamma$	0 (0, 0)	0 (0, 0)	0 (0, 0)	0 (0, 0)
Invisible	— (—, —)	— (—, —)	0 (0, 14.9)	0 (0, 20.3)
All	20.8 (31.3, 1.4)	40.8 (53.6, 9.5)	99.96 (100.0, 100.0)	100.0 (100.0, 100.0)

Table 5: Same as Table 4 above but now for the subset of models expected to remain after the ATLAS 14 TeV zero lepton jets + MET search with 300 fb⁻¹ of data.

Channel	300 fb ⁻¹ LHC	3 ab ⁻¹ LHC	500 GeV ILC	HL 500 GeV ILC
$b\bar{b}$	20.1 (30.9, 0)	39.1 (53.0, 66.7)	83.2 (94.1, 66.7)	93.5 (97.9, 100.0)
$\tau\tau$	0.7 (0.7, 0)	3.3 (2.8, 66.7)	14.3 (9.9, 66.7)	40.9 (33.9, 66.7)
$g\bar{g}$	0 (0, 0)	0 (0, 33.3)	100.0 (100.0, 100.0)	100.0 (100.0, 100.0)
$\gamma\gamma$	0 (0, 0)	0 (0, 0)	0 (0, 0)	0 (0, 0)
Invisible	— (—, —)	— (—, —)	0 (0, 0)	0 (0, 0)
All	20.4 (31.1, 0)	40.1 (54.0, 66.7)	100.0 (100.0, 100.0)	100.0 (100.0, 100.0)

Table 6: Same as Table 4 above but now for the subset of models expected to remain after the ATLAS 14 TeV zero lepton jets + MET search with 3 ab⁻¹ of data.

5 Conclusion

In this White Paper we have examined SUSY signals and Higgs boson properties in the context of the pMSSM in models with either neutralino or gravitino LSPs and in models with low FT. Within this general scenario we then addressed the following questions: ‘What will potentially null searches for SUSY at the LHC tell us about the possible properties of the Higgs boson?’ and, conversely, ‘What do precision measurements of the properties of the Higgs tell us about the possible properties of the various superpartners?’ We again warn the reader that in obtaining the results presented here we have ignored any theoretical errors associated with the calculation of the Higgs coupling ratios as given by HDECAY. Our results can be further refined once a better understanding of this uncertainty is provided by future theoretical work.

We saw in the above discussion that the answer to the first question was rather straightforward: Given an initial distribution of signal strengths μ_X or branching fraction ratios r_X for a specific final state, the LHC direct SUSY searches reduce the size of the distribution but to a very good approximation do not change its *shape*. This was shown to be true for all three model sets. This implies that to first order the direct (null) SUSY searches at the LHC will not impact the range of possible deviations of Higgs branching fractions from their SM values. This is a very powerful result.

However, we found the answer to the second question to be much more complex and of potentially even greater importance: Precision measurements of Higgs couplings and branching fractions can lead to the exclusion of pMSSM models which cannot be probed by the powerful 14 TeV zero lepton, jets plus MET search, even with an integrated luminosity of 3 ab^{-1} . This is true for all model sets and also true whether or not the precise values of the measured quantities are consistent with the SM expectation. Of course, the more precisely the Higgs couplings are measured, the greater the fraction of pMSSM models that can be probed. Since the $hb\bar{b}$ coupling can deviate the furthest from its SM value within the pMSSM framework, measurements of its value generally have the greatest impact *if* we do not assume that the central values measured for the Higgs couplings are given exactly by their SM values. If this is the case, however, then the hgg coupling at the ILC will provide the strongest constraint as this quantity is necessarily shifted in the pMSSM by stop loops with a central value crudely determined by the necessity of obtaining the correct Higgs mass. In such a case (or if the observed central values for r_{gg} – or to a lesser extent $r_{\gamma\gamma}$ – differ from the SM in the opposite direction from the pMSSM prediction), essentially all of the pMSSM parameter space considered here would then be excluded.

6 Acknowledgments

We wish to thank M. Spira for answering our many questions and for assistance with the implementation of the latest version of HDECAY. This work was supported by the Department of Energy, Contract DE-AC02-76SF00515.

References

- [1] For an overview of MSSM physics and phenomenology as well as mSUGRA, see M. Drees, R. Godbole, P. Roy, Hackensack, USA: World Scientific (2004) 555 p; H. Baer, X. Tata, Cambridge, UK: Univ. Pr. (2006) 537 p; S. P. Martin, In *Kane, G.L. (ed.): Perspectives on supersymmetry II* 1-153 [hep-ph/9709356].
- [2] T. Cohen and J. G. Wacker, arXiv:1305.2914 [hep-ph].
- [3] See, for example, A. Armbruster, ATLAS Collaboration, talk given at *Recontres de Moriond: QCD and High Energy Interaction*, LaThuile, March 9-16, 2013.
- [4] See, for example, N. Wardle, CMS Collaboration, talk given at *Recontres de Moriond: QCD and High Energy Interaction*, LaThuile, March 9-16, 2013.
- [5] A. Djouadi *et al.* [MSSM Working Group Collaboration], hep-ph/9901246; C. F. Berger, J. S. Gainer, J. L. Hewett and T. G. Rizzo, JHEP **0902** (2009) 023 [arXiv:0812.0980 [hep-ph]].
- [6] M. W. Cahill-Rowley, J. L. Hewett, S. Hoeche, A. Ismail and T. G. Rizzo, Eur. Phys. J. C **72**, 2156 (2012) [arXiv:1206.4321 [hep-ph]].
- [7] M. W. Cahill-Rowley, J. L. Hewett, A. Ismail and T. G. Rizzo, Phys. Rev. D **86**, 075015 (2012) [arXiv:1206.5800 [hep-ph]], Phys. Rev. D **88**, 035002 (2013) [arXiv:1211.1981 [hep-ph]], arXiv:1211.7106 [hep-ph] and in preparation.
- [8] E. Komatsu *et al.* [WMAP Collaboration], Astrophys. J. Suppl. **192**, 18 (2011) [arXiv:1001.4538 [astro-ph.CO]].
- [9] B. C. Allanach, Comput. Phys. Commun. **143**, 305 (2002) [hep-ph/0104145].
- [10] A. Djouadi, J. L. Kneur and G. Moultaka, Comput. Phys. Commun. **176**, 426 (2007) [arXiv:hep-ph/0211331].
- [11] A. Djouadi, M. M. Muhlleitner and M. Spira, Acta Phys. Polon. B **38**, 635 (2007) [hep-ph/0609292].
- [12] Thanks to M. Spira, we employed HDECAY 5.11 in the present analysis which can be obtained from <http://people.web.psi.ch/spira/hdecay/>. For the original reference, see A. Djouadi, J. Kalinowski and M. Spira, Comput. Phys. Commun. **108**, 56 (1998) [hep-ph/9704448].
- [13] M. Cahill-Rowley, J. L. Hewett, A. Ismail and T. G. Rizzo, arXiv:1307.8444 [hep-ph]; M. Cahill-Rowley, R. Cotta, A. Drlica-Wagner, S. Funk, J. Hewett, A. Ismail, T. Rizzo and M. Wood, arXiv:1305.6921 [hep-ph].

- [14] J. R. Ellis, K. Enqvist, D. V. Nanopoulos and F. Zwirner, *Mod. Phys. Lett. A* **1**, 57 (1986).
- [15] R. Barbieri and G. F. Giudice, *Nucl. Phys. B* **306**, 63 (1988).
- [16] J. A. Conley, J. S. Gainer, J. L. Hewett, M. P. Le and T. G. Rizzo, *Eur. Phys. J. C* **71** (2011) 1697 [arXiv:1009.2539 [hep-ph]] and [arXiv:1103.1697 [hep-ph]].
- [17] S. Chatrchyan *et al.* [CMS Collaboration], *Phys. Lett. B* **713**, 408 (2012) [arXiv:1205.0272 [hep-ex]]; S. Chatrchyan *et al.* [CMS Collaboration], *Phys. Lett. B* **713**, 68 (2012) [arXiv:1202.4083 [hep-ex]].
- [18] R. Aaij *et al.* [LHCb Collaboration], arXiv:1307.5024 [hep-ex]; S. Chatrchyan *et al.* [CMS Collaboration], arXiv:1307.5025 [hep-ex]. The analysis as presented here, however, employs the earlier results as given in R. Aaij *et al.* [LHCb Collaboration], *Phys. Rev. Lett.* **110**, 021801 (2013) [arXiv:1211.2674 [Unknown]]. The numerical impact of these later results on our analysis is very minor.
- [19] T. Sjostrand, S. Mrenna and P. Z. Skands, *JHEP* **0605**, 026 (2006) [hep-ph/0603175].
- [20] J. Conway, PGS4, Pretty Good detector Simulation, <http://www.physics.ucdavis.edu/~conway/research/software/pgs/pgs.html> .
- [21] W. Beenakker, R. Hopker, M. Spira and P. M. Zerwas, *Nucl. Phys. B* **492**, 51 (1997) [arXiv:hep-ph/9610490];
- [22] The Higgs coupling results from ATLAS based on 7 and 8 TeV data can be found at <https://twiki.cern.ch/twiki/bin/view/AtlasPublic/HiggsPublicResults>, while those from CMS can be found at <https://twiki.cern.ch/twiki/bin/view/CMSPublic/PhysicsResultsHIG>.
- [23] We employ the results as presented by ATLAS in ATL-PHYS-PUB-2012-004 and by CMS as presented by J. Olsen at the *Snowmass Energy Workshop*, U. of Washington, Seattle, 7/1/2013. In the numerical analysis presented here, we make explicit use of these projected CMS Higgs coupling results for the 14 TeV LHC assuming the larger error for both luminosities.
- [24] We follow the results as presented by M. E. Peskin, arXiv:1207.2516 [hep-ph]; M. Klute, R. Lafaye, T. Plehn, M. Rauch and D. Zerwas, *Europhys. Lett.* **101**, 51001 (2013) [arXiv:1301.1322 [hep-ph]]; The ILC Technical Design Report: Vol.2, H. Baer *et al.*, 2013. Here we make explicit use of the Higgs coupling analysis results as presented in ‘ILC Higgs White Paper’, D. Asner *et al.*, submitted to Snowmass 2013.
- [25] M. Carena, S. Gori, N. R. Shah, C. E. M. Wagner and L. -T. Wang, arXiv:1303.4414 [hep-ph].
- [26] A. Djouadi, L. Maiani, G. Moreau, A. Polosa, J. Quevillon and V. Riquer, arXiv:1307.5205 [hep-ph].